Published in final edited form as:

*Theriogenology*. 2019 March 15; 127: 41–48. doi:10.1016/j.theriogenology.2018.12.031.

# Bovine eggs release zinc in response to parthenogenetic and sperm-induced egg activation

**Emily L. Que**[a], **Francesca E. Duncan**[b], **Lee Hoi Chang**[b], **Jessica E. Hornick**[b], **Stefan Vogt**[c], **Rafael A. Fissore**[d], **Thomas V. 0'Halloran**[a,e,f], **Teresa K. Woodruff**[a,b,f]

[a]The Chemistry of Life Processes Institute, Northwestern University, Evanston, IL, 60208, USA

[b]Department of Obstetrics and Gynecology, Feinberg School of Medicine, Northwestern University, Chicago, IL, 60611, USA

[c]X-ray Sciences Division, Argonne National Laboratory, Argonne, IL, 60439, USA

[d]Department of Veterinary and Animal Sciences, University of Massachusetts, Amherst, MA, 01003, USA

[e]Department of Chemistry, Northwestern University, Evanston, IL, 60208, USA

[f]Department of Molecular Biosciences, Northwestern University, Evanston, IL, 60208, USA

## Abstract

Upon fertilization or parthenogenesis, zinc is released into the extracellular space through a series of exocytic events termed zinc sparks, which are tightly coordinated with intracellular calcium transients. The zinc spark reduces the total amount of intracellular zinc, and this reduction is necessary and sufficient to induce egg activation even in the absence of calcium transients. In addition, this zinc release contributes to the block to polyspermy through modification of the zona pellucida. The zinc spark has been documented in all organisms examined to date including the mouse, two species of nonhuman primates, and human. Here we determined whether zinc sparks occur in the bovine, an important model of gamete development in mono-ovulatory mammalian species. We obtained metaphase ll-arrested (MII) bovine eggs following in vitro maturation. Total zinc, assessed in single cells using X-Ray Fluorescence Microscopy, was significantly more abundant in the bovine egg compared to iron and copper. Studies with intracellular fluorescent probes revealed that labile zinc pools are localized to discrete cytoplasmic punctae enriched at the cortex. To determine whether zinc undergoes dynamic fluxes during egg activation, we parthenogenetically activated bovine eggs using two approaches: ionomycin or bovine phospholipase C zeta (bPIcζ). Both these methods induced zinc sparks coordinately with intracellular calcium transients. The zinc spark was also observed in bovine eggs following intracytoplasmic sperm injection. These results establish that zinc is the most abundant transition

Authors' Roles

EQ, FD, and HL contributed equally to the conception and design of experiments, acquisition and analysis of data, writing and revision of the article, and final approval of the article. JH and SV contributed to the acquisition of data and final approval of the article. RF, TO, and TW contributed to the conception and design of experiments, interpretation of the results, revision of the article, and final approval of the article.

Declarations of interest

None.

metal in the bovine egg, and zinc flux during egg activation - induced by chemical activation or sperm - is a highly conserved event across mammalian species.

## 1. Introduction

Coordinated fluctuations in concentration and localization of zinc ions ($Zn^{2+}$), like calcium ions ($Ca^{2+}$), play central roles in oocyte maturation, fertilization, and embryogenesis [[1], [2], [3], [4], [5], [6], [7], [8], [9], [10], [11], [12], [13], [14], [15], [16], [17], [18], [19], [20], [21]]. In the mouse model, zinc is the most abundant transition metal in the female gamete, and the total cellular $Zn^{2+}$ content in the egg increases by ca. 20 billion atoms (a 50% increase) as it progresses from the prophase I arrest (oocyte) to the arrest at metaphase of meiosis II (M II, egg). Following fertilization, total $Zn^{2+}$ content decreases by ca. 12 billion atoms (a 20% decrease) [5]. $Zn^{2+}$ influx during meiosis is required to advance the oocyte through anaphase by binding the $Zn^{2+}$-dependent factor Emi2 [2].

Subsequent efflux of $Zn^{2+}$ signals a transition between the meiotic and mitotic cell cycle, and artificially lowering $Zn^{2+}$ availability at the MII stage results in parthenogenetic activation in multiple species including the mouse, nonhuman primate, and human [3,4,10,17], $Zn^{2+}$ loss from the Mil egg at fertilization is achieved through the exocytosis of thousands of $Zn^{2+}$-enriched cortical vesicles in a biological process we have termed the ‘zinc spark’ [4,9], The high micromolar concentration of $Zn^{2+}$ released at fertilization not only regulates the activity of the cell cycle regulator Emi2, but $Zn^{2+}$ exocytosis causes zona hardening and prevention of polyspermy in mice [20,21], Studies in the murine model demonstrate that the $Zn^{2+}$ release measured immediately after fertilization can be correlated with embryo development - with higher amplitude zinc sparks corresponding to better quality embryos [14]. $Zn^{2+}$ is also critical for preimplantation embryo development where it has been implicated in mitotic cell division and chromatin configuration and transcriptional regulation [8].

While the mouse has been one of the most common model systems for studying $Zn^{2+}$ fluxes in the context of the reproductive biology of eggs and embryos, the bovine is an attractive model system for several reasons. First, the bovine is mono-ovulatory and has a longer lifespan relative to the mouse. Second, bovine ovaries are similar to human ovaries with respect to size, architecture, and follicle distribution within the tissue. Third, there are parallel follicle development patterns in the bovine and human, including distinct follicular and luteal phases and similar endocrine profiles, especially with respect to inhibin [22,23], Finally, there are parallels in bovine and human egg biology in regards to the size of the egg [24,25], the morphology and positioning of the meiotic spindle [[26], [27], [28]], and features of the zona pellucida are also similar [29,30].

Existing studies investigating $Zn^{2+}$ roles in the bovine ovary and oocyte suggest that this transition metal may have an important function in these reproductive tissues and cells. X-ray Fluorescence Microscopy (XFM), a technique that can be used to quantify and visualize the metal content of biological samples, demonstrated that bovine ovarian tissue, including follicles, contains Cu, Fe, Zn, Se, and Br [31,32], Furthermore, other studies suggest that supplementation of in vitro maturation media with $Zn^{2+}$ can improve fertilization and

preimplantation embryo outcomes following in vitro fertilization [33,34], The goal of this work is to further characterize $Zn^{2+}$ in the bovine egg and determine whether it undergoes dynamic changes during fertilization using state-of-the-art probes and imaging modalities. Employing the bovine model system to evaluate models for the roles of zinc fluxes in regulation of fertility will advance our knowledge of the basic biology of fertilization in large monovulatory mammalian species and is directly relevant to both livestock husbandry and human Assisted Reproduction Technologies (ART).

## 2. Materials and methods

### 2.1. Bovine gamete collection and in vitro maturation (IVM)

Bovine ovaries were obtained from Aurora Packing Company (Aurora, IL) and transported in prewarmed BoviPRO Oocyte Holding Media (1182/1210, MOFA, Verona, WI) by courier service to Northwestern University within 2 h of slaughter. The Aurora Packing Company is an abattoir that processes cattle from multiple sites across the Midwest within a 300 mile radius of Chicago. Thus, we were unable to control the source of the material we received for our studies. However, the majority of samples are from beef cattle (Angus breed), and the heifers are post-pubertal and reproductively adult (between 24 and 30 months). Immediately upon arrival, COCs were harvested from whole ovaries by slashing small antral follicles (3–6 mm) with a scalpel directly into Oocyte Holding Media. The media was then passed through a 70 μm mesh filter to remove small cells. COCs were then rinsed off the mesh, and only intact and healthy appearing COCs were selected for further IVM. Unhealthy appearing COCs and denuded oocytes were avoided. For IVM, COCs were transferred to BoviPRO Oocyte Shipping and Maturation Media (19982/1231, MOFA) with 20 COCs added per vial. The media was overlaid with 500 μI of mineral oil, and IVM was performed at 39 °C for specified times. For the IVM time course, IVM was performed for between 4 and 24 h. For all other experiments, IVM was performed for between 22 and 24 h. Following IVM, COCs were removed from each vial and cumulus cells were removed either mechanically or by a brief incubation in Oocyte Holding Media supplemented with 3 mg/ml hyaluronidase (Sigma-Aldrich, St. Louis, MO). Transmitted light images were taken using a Leica DM IRB inverted microscope (Leica Microsystems, Heidelberg, Germany). Cells were then used for live imaging experiments as described below. To obtain diameter measurements, transmitted light images of cells at each stage of meiosis were taken, and ImageJ software [35] was used to take two perpendicular diameter measurements from plasma membrane-to-plasma membrane. The average diameter per oocyte was reported.

### 2.2. Whole mount immunocytochemistry

Cells were fixed in 3.8% paraformaldehyde (Electron Microscopy Sciences, Hatfield, PA) containing 0.1% Triton-X-100 (Sigma-Aldrich, St. Louis, MO) at 1 h at 37 °C. Cells were rinsed briefly in phosphate buffered saline (PBS) containing 0.3% bovine serum albumin (BSA) (MP Biomedicals, Santa Ana, CA) and 0.01% Tween-20 (Sigma-Aldrich, St. Louis, MO) (blocking buffer) and permeabilized for 30 min in PBS containing 0.3% BSA and 0.1% Triton X-100. Eggs were incubated in mouse anti-bovine alpha-tubulin antibody (A11126; Life Technologies, Carlsbad, CA, 1:50 dilution) overnight at 4 °C, rinsed in blocking buffer, and then incubated in donkey anti-mouse Alexa Fluor 488 (Life Technologies, Carlsbad,

CA; 1:100 dilution) and rhodamine-phalloidin (Life Technologies, Carlsbad, CA; 1:50 dilution). Cells were then rinsed in blocking buffer and mounted in Vectashield containing DAPI (Vector Laboratories, Burlingame, CA). Immunofluorescence was visualized using a Leica SP5 inverted laser scanning confocal microscope (Leica Microsystems, Heidelberg, Germany) using 405 nm, 488 nm, and 543 nm lasers.

### 2.3. Synchrotron-based x-ray fluorescence microscopy (XFM)

Bovine eggs were collected as described above and cells that displayed a clear polar body and were completely free from cumulus cells were selected for XFM analysis. Cells were washed into 100 mM NH40Ac buffer and air-dried onto SiN windows (Silson, Warwickshire, England). XFM was performed at Beamline 2-ID-E at the Advanced Photon Source (Argonne National Laboratory). With a singlebounce Si(111) monochromator, 10-keV X-rays were monochromatized and focused to a spot size of 0.5 × 0.6 μm using Fresnel-zone plate optics (X-radia, Pleasanton, CA). Fly scans were done in steps of 0.3 μm. Fluorescence spectra were collected with a 30 ms dwell time using a silicon drift detector (Vortex-EM, Hitachi, Northridge, CA). Per pixel spectrum fitting was performed using MAPS [36]. The elemental concentration in μg/cm2 was determined by comparing the signal intensity of the samples with that from an AXO standard (RF8–2000s2453), i.e. a thin film with known elemental concentration, under the same experimental condition. For thin sections, μg/cm2 values were converted to per volume concentration by taking into account the known sample thickness.

### 2.4. Intracellular labile $Zn^{2+}$ imaging

Bovine eggs were incubated in 5 pM FluoZin-3-AM and 0.2% Pluronic® F-127 for 30 min prior to imaging. Fluorescence images were obtained using 488 nm laser excitation on a Leica SP5 confocal microscope. Following initial imaging, the same cells were incubated in 10 μM TPEN for 30 min and were re-imaged using the same imaging conditions.

### 2.5. Fluorescence monitoring of activation with Ca-ionomycin

Activation with Ca-ionomycin was carried out in Ca-free Hepes-buffered CZB (HCZB, Chatot, Ziomek, and Bavister) medium and was monitored using a Leica SP5 confocal microscope. FluoZin-3 acid (50 μM) was used to monitor extracellular $Zn^{2+}$ and either Fluo-4-AM or Fura-2-AM (5 μM) was used to monitor intracellular $Ca^{2+}$. Cells were incubated with a mixture of $Ca^{2+}$probe and 0.2% F124 Pluronic® (Life Technologies, Carlsbad, CA) for 30 min at 37 °C. For imaging, cells were placed at one end of a 360 μL oblong droplet of HCZB containing FZ3 in a Fluorodish® (WPI Inc., Sarasota, FL) at 37 °C under mineral oil. After focusing, a 40 μL aliquot of Ca-ionmycin in DMSO/HCZB was added to give a final concentration of 50 μM. Images were taken every 2–3 s using a 405 nm laser for Fura-2 excitation and/or a 488 nm laser for Fluo-4 and/or FluoZin-3 excitation. Image analysis was performed using ImageJ.

### 2.6. Fluorescence monitoring of activation with bovine PLC-ζ (bPLC-ζ)

Full-length bPLC-ζ was kindly provided by Dr. Nancy D'Cruz (Monash Institute, Melbourne, Australia). bPLC-ζ was subcloned into the pGEM tEASY 3.1 vector between

the Apal and Sail restriction sites. To generate cRNA, the plasmid was linearized and in vitro transcribed using the T7 mMESSAGE mMACHINE kit (Ambion, Austin, TX) according to the manufacturer's instructions. Then, a poly-A tail was added to the cRNA using the Poly-A tail kit (Ambion, Austin, TX). cRNA was purified using the MEGA clear kit (Ambion, Austin, TX), and stored at −80 °C in use aliquots. Microinjection techniques were carried out as described [37], In brief, bovine eggs were microinjected using Narishige manipulators mounted on a Nikon diaphot microscope (Nikon). Glass micropipettes filled by suction of a microdrop containing 0.5 μg/μl bPLC-ζ cRNA and injected into the cytoplasm by pico-injector (PLI-100, Harvard Apparatus, Cambridge, MA). Injection volumes ranged from 15 to 20 pl in bovine eggs. All injections were carried out at room temperature in TL-HEPES 5% FCS and 2.5% sucrose. Before injection, bovine eggs were centrifuged in TL-HEPES at 5000×g for 8 min to allow for easier visualization of the injection. All eggs injected with bPLC-ζ cRNA were incubated for 1 h prior to initiating fluorescence imaging to allow for sufficient protein expression. Bovine eggs were injected with the fluorescent dye Fura-2 dextran (Life Technologies, Carlsbad, CA) at room temperature. $Ca^{2+}$ imaging was carried out as described [38]. In brief, excitation wavelengths were at 340 and 380 nm and the emitted light was quantified, after passing through a 510 nm barrier filter. Neutral density filters attenuated the intensity of the excitation light, and the fluorescent signal was averaged for the whole cell. Eggs were monitored in groups of 6–9 in 200 μl drops of TL-HEPES on a glass bottom dish (MatTek Corp., Ashland, MA) under mineral oil. Fluorescence ratios were taken every 10–20 s for various time points depending on the experiment. Time laps image files were then transported to numeric values reported as the ratios of 340/380 nm fluorescence. Files were imported to Microsoft Excel and representative $Ca^{2+}$ traces were graphed as the ratio of 340/380 nm fluorescence.

### 2.7. Fluorescence monitoring of activation following intracytoplasmic sperm injection (ICSI)

Bovine sperm was purchased from commercially available frozen spermatozoa (Cattle Visions, MO. USA) from a bull with proven fertility, thawed, and separated using a 45%, 90% Isolate gradient (Irvine Scientific, CA. USA). These spermatozoa (5 × 106 spermatozoa/mL) were then washed in Sperm-Tyrode's albumin lactate pyruvate (Sp-TALP) medium [39] for 5 min and then used for ICSI as previously described [40,41] using Eppendorf manipulators (Eppendorf TransferMan NK2, Hamburg, Germany) mounted on a Nikon Eclipse TE300 microscope (Nikon Inc., Garden City, NY). Before ICSI, bovine eggs were centrifuged in TL-HEPES at 5000×g for 8 min to allow for easier visualization of sperm injection. ICSI was performed in HCZB medium [42] at room temperature using bovine MII eggs obtained following IVM. The bovine sperm were sonicated to decapitate the heads [43]; sonication (B2500A-MTH, VWR, Radnor, PA) was carried out for 20 s at 4 °C. The sperm suspension was mixed in a ratio of 1:1 with injection buffer containing 12% polyvinyl pyrrolidone (PVP, M.W. 360 kDa; Sigma).

The working concentration was 6% PVP with sperm. Sperm was delivered into the egg cytosol using a PMM (Piezo Micromanipulator, Prime Tech LTD. Japan) with an Eppendorf injection pipette (Piezo Drill Tip Mouse ICSI, Eppendorf, Hamburg. Germany). After ICSI, sperm injected eggs were transferred to a glass bottom dish to monitor zinc and calcium

[44], Fura 2-AM dye was excited between 340 nm and 380 nm, and FluoZin-3 was excited at 488 nm by a filter wheel (Lambda 10–3, Sutter Instrument), and fluorescence was captured every 10 s.

### 2.8. Statistical analysis

Statistical tests (ANOVA) were performed using the software Prism 5.0 (GraphPad). $P < 0.05$ was considered statistically significant.

## 3. Results

### 3.1. Bovine eggs contain high amounts of $Zn^{2+}$, with labile $Zn^{2+}$ localized to cortical vesicles

To obtain mature bovine eggs for zinc analysis and egg activation studies, we performed in vitro maturation (IVM) of cumulus oocyte complexes isolated from small antral follicles from bovine ovaries harvested at a local abattoir. We first performed a time course to determine the time post-IVM where there were maximum numbers of mature MII eggs as confirmed by chromatin configuration analysis. The majority of mature eggs were observed at 22–24 h post-IVM, with >40% of the cells arrested at MII (Fig. 1A). Oocytes exhibited a size-dependent ability to progress through meiosis. Cells that reached MII had a diameter of 124.1 ± 10.1 μm, whereas those that failed to resume meiosis and were arrested in prophase I were significantly smaller ($p < 0.004$) with an average diameter of 113.1 ±10.6 μm, (Fig. 1B). MII-arrested eggs obtained through IVM had characteristic morphology, including enrichment of cortical actin, an asymmetrically positioned meiotic spindle with chromosomes tightly aligned on the metaphase plate, and a small polar body (Fig. 1C). Using this cell population, we performed XFM to determine the elemental composition of the bovine egg (Fig. 2). Individual MII eggs obtained following IVM (n = 13) were mounted for analysis. This technique enables quantitation of the total metal ion pool, which consists of labile (loosely bound) metals as well as metals tightly bound to proteins, membranes etc. Similar to our observations in the mouse, bovine MII eggs contained significantly more Zn relative to Fe and Cu (Fig. 2A and B) [5,9]. Specifically, there were 1.4 (±0.7) × 1011 atoms of Zn, 2.6 (±1.4) × 1010 atoms of Fe, and 1.5 (±0.9) × 1010 atoms of Cu in the bovine MII egg (Fig. 2B). In all samples examined, total Fe, Cu, and Zn localized throughout the cytoplasm in a uniform fashion (Fig. 2A), which is in contrast to the hemispherical total Zn distribution pattern observed in mouse eggs which have a prominent polarity at this stage of meiosis unlike bovine eggs [4].

To examine the distribution of labile $Zn^{2+}$ in bovine MII eggs, we performed live cell imaging using the cell-permeable $Zn^{2+}$-responsive fluorophore, FluoZin-3-AM. Labile Zn localized to discrete punctate structures at the cell periphery (Figure C, white arrow). The fluorescence signal was depleted following treatment with the heavy metal chelator N,N,N',N'-tetrakis(2-pyridylmethyl)ethane-1,2-diamine (TPEN) that has high affinity for $Zn^{2+}$, suggesting that observed fluorescence is specific to $Zn^{2+}$ and not simply due to dye accumulation (Fig. 2D) [4,9,45]. These data indicate that labile $Zn^{2+}$ in bovine eggs is sequestered in cortical compartments. These $Zn^{2+}$-enriched vesicles are analogous to the

$Zn^{2+}$-enriched cortical vesicles that have been observed in mouse and human eggs [4,7,9], and have recently been shown to be part of cortical granules in mice [21].

### 3.2. Ionomycin treatment induces a single zinc spark in bovine eggs

Fertilization and the activation of embryonic development in the bovine is triggered by a series of long-lasting oscillations of intracellular free calcium [$Ca^{2+}$]i [37], The pattern of [$Ca^{2+}$]i oscillations is species-specific, and in bovine these oscillations have been observed to occur over a 16–18 h time period. Treatment with ionomycin can be used to activate bovine eggs parthenogenetically. Ionomycin is a $Ca^{2+}$ ionophore that induces a single large rise in cytosolic $Ca^{2+}$ concentration due to delivery of exogenous $Ca^{2+}$into the cell and/or release of intracellular $Ca^{2+}$ stores [46].

To probe the relationship between intracellular $Ca^{2+}$ ([$Ca^{2+}$]i) and extracellular $Zn^{2+}$ dynamics during bovine egg activation, we simultaneously monitored intracellular $Ca^{2+}$ (Fluo-4-AM or Fura-2-AM) and extracellular $Zn^{2+}$ (FluoZin-3) following activation with Ca-ionomycin (ionomycin pre-bound with $Ca^{2+}$) (Fig. 3A and B, Video S1). Exposure to ionomycin in the presence of extracellular $Ca^{2+}$, which is how this ionophore is routinely used in bovine oocytes, causes influx of exogenous $Ca^{2+}$ into the cells in addition to release of intracellular stores. As expected, after the addition of Ca-ionomycin, a rise in [$Ca^{2+}$]i was observed concurrently with an increase in extracellular $Zn^{2+}$ (N = 22 eggs) (Fig. 3A and B). Thus, consistent with what we have observed in mouse and human eggs, there is a correlation between $Ca^{2+}$ signaling and the zinc spark in bovine eggs as well [3,4].

To exclude any potential artifacts from intracellular dye treatment, we monitored $Zn^{2+}$ exocytosis in response to ionomycin-induced egg activation using only FluoZin-3, which does not go into the cell in this form because it is not modified with acetoxymethyl (AM) esters (Fig. 3C and D, Video S2). The zinc spark was observed using only extracellular FluoZin-3, demonstrating that the fluorescence signal is due specifically to $Zn^{2+}$ exocytosis (Fig. 3C). We observed a high degree of variability in the intensity of zinc sparks among eggs (total N = 32), with some not exhibiting a spark (N = 4) and others having low (N = 14), medium (N = 13), and high (N = 1) zinc spark intensity profiles (Fig. 3D). This heterogeneity has been observed previously in mouse and human eggs and suggests potential underlying differences in egg quality [3,14].

### 3.3. PLC-ζ activation and intracytoplasmic sperm injection (ICSI) induce zinc sparks in bovine eggs

While ionophore treatment is a convenient method to induce rises in [$Ca^{2+}$]i, it bypasses endogenous $Ca^{2+}$ stores in the egg. To test if zinc sparks can be induced using a more physiologic approach, we activated eggs using bPLC-ζ cRNA (Fig. 4). This method induces [$Ca^{2+}$]i oscillations, downregulates the IP3 receptor, and supports high rates of parthenogenesis [41]. Extracellular $Zn^{2+}$ was monitored with FluoZin-3, and [$Ca^{2+}$]i was monitored in a subset of eggs using Fura-dextran because this impermeable dye is necessary to monitor [$Ca^{2+}$]i over prolonged time periods. In 9 of the 12 eggs monitored, we observed between 1 and 3 zinc sparks; 3 eggs did not produce observable zinc sparks (Fig. 4). In eggs

that were monitored for both $Ca^{2+}$ and $Zn^{2+}$, zinc sparks immediately followed rises in $[Ca^{2+}]i$.

To examine whether sperm-induced egg activation could elicit the zinc spark, we attempted in vitro fertilization (IVF). While bovine IVF performed under optimal conditions (media, temperature, gas) in our hands resulted in 49% of the fertilized zygotes cleaving to the 2-cell stage, bovine IVF was not successful when performed under the conditions required to monitor the zinc spark, which requires fluorescence microscopy (data not shown). To overcome this technical limitation, we performed ICSI whereby fertilization is induced through microinjection of sperm directly into the cytoplasm of the egg. In general, ICSI is not efficient in the bovine system, so we had to inject multiple sperm into a single egg to trigger egg activation. However, when egg activation was successful as evidenced by a rise in $[Ca^{2+}]i$., we observed a corresponding zinc spark (Fig. 5). Taken together, these results demonstrate that zinc sparks are a hallmark of bovine egg activation that can be induced by multiple parthenogenetic methods as well as sperm. The zinc spark is a highly conserved event during egg activation in all large mammalian species examined to date.

## 4. Discussion

The egg-to-embryo transition requires events collectively referred to as egg activation, including completion of meiosis, zona pellucida modification, pronuclear formation, and maternal mRNA recruitment [47], Cytoplasmic $[Ca^{2+}]i$ transients in the egg, triggered by sperm PLC-ζ, are important for activating downstream signaling molecules involved in egg activation [[48], [49], [50], [51]]. Distinct $[Ca^{2+}]i$ oscillatory patterns dictate specific events of egg activation and are directly related to embryo quality [[52], [53], [54]]. For example, fertilized post-ovulatory aged eggs, which have reduced developmental competence, have altered $[Ca^{2+}]i$ profiles compared to controls [55,56]. Zinc sparks and intracellular $[Ca^{2+}]i$ transients are linked, with $[Ca^{2+}]i$ rises immediately preceding rises in extracellular $Zn^{2+}$ [4], As such, extracellular $Zn^{2+}$ may be a viable surrogate for $[Ca^{2+}]i$ and we have previously demonstrated a link between zinc spark intensity following egg activation and blastocyst quality [14].

While most previous studies have focused on mouse, the results presented here expand these studies to bovine. Similar to mouse eggs, the bovine egg contains an order of magnitude more total Zn than either Fe or Cu; this unusual metal content ratio implies a similar role for zinc in bovine eggs as in mouse. The total Zn content of the bovine MII egg was ~2.5 times greater than what we observed in the mouse MII egg [5], consistent with the larger volume of the bovine egg. Labile zinc is localized to cortical vesicles in both species, and data in mouse indicates that these structures are cortical granules or a subset thereof [9,21], In mouse eggs, both total and labile $Zn^{2+}$ have an asymmetric distribution in MII eggs, the pattern of which is quite similar to the polarized distribution of cortical granules, and the substantial cortical granule free domain (CGFD) in this cell type [4,9]. Both human and bovine eggs, on the other hand, display a uniform distribution of total and labile $Zn^{2+}$, consistent with the lack of prominent polarity and CGFD in both bovine and human eggs ([3] and unpublished).

Here we report for the first time that bovine eggs undergo activation-induced zinc sparks similarly to murine, nonhuman primate, and human species, as both Ca-ionomycin and PLC-ζ activation methods as well as sperm induce $Zn^{2+}$ release from these cells. The zinc spark profiles of individual eggs varied, suggesting underlying differences in quality. This variability is observed in mouse [14] and human [3] as well, but is more pronounced in human and bovine than in mouse. This may have origins in how eggs are collected in each species. In mouse studies, MII eggs were collected from reproductively young mice that were housed in controlled research facilities and were primed with gonadotropins, making the population of eggs uniform in quality [4,9,14], Human eggs used for zinc spark studies, however, were collected from IVF patients and were received at various meiotic stages [3], Thus, the samples had greater variability in terms of origin and once received, eggs underwent IVM until the MII stage was achieved. In this study, bovine eggs were obtained from whole ovaries following isolation of COCs from small antral follicles and then were matured in vitro. Thus, in both the human and bovine studies, IVM was used to obtain eggs meiotically competent for activation. Several studies demonstrate how IVM impairs the quality of MII eggs, resulting in defects in spindle formation, production of cytoplasmic components important for cell cycle regulation, and exocytosis of cortical granules [[57], [58], [59]]. In addition, there was heterogeneity in our bovine samples with respect to potential differences in animal breed, age, diet (especially with respect to zinc content), and fertility status, which may impact the zinc spark profile. Future studies in more controlled animal populations would be of significant value.

Consistent with previous studies [3,4], zinc sparks in bovine display tight temporal coordination with intracellular $[Ca^{2+}]$i transients during both Ca-ionomycin and bPLC-ζ-induced egg activation. The number of sparks varies in all of the activation methods. Ca-ionomycin activation produces a single $[Ca^{2+}]$i transient and a single zinc spark in all species studied to date [3,4], SrCI2 activation in mouse, which induces repetitive $[Ca^{2+}]$i transients, induces between one and five zinc sparks per egg [4], It is worth noting that we were unable to use SrCI2 to monitor zinc sparks in bovine or human eggs, as it does not causes oscillations in the eggs of these species [60]. PLC-ζ activation in human and bovine produced fewer zinc sparks despite inducing multiple $[Ca^{2+}]$i transients. Since introduction of exogenous PLC-ζ induces activation that most closely mimics fertilization-induced $[Ca^{2+}]$i transients [61], this finding is consistent with previous results in mouse eggs, where IVF-activation on average results in fewer zinc sparks than SrCI2 activation [4,14], In human, only one zinc spark is observed following hPLC-ζ activation. In bovine, on the other hand, between one and three zinc sparks are observed following bPLC-ζ activation. The zinc spark has been observed in response to sperm during the process of IVF in mice demonstrating that this biological process is not an artifact of parthenogenetic activation methods [14,21], Unfortunately, we were not able to successfully monitor calcium and zinc during bovine IVF due to technical limitations, but we did observe the zinc spark following ICSI. Determining the precise activation-dependent patterns of the zinc spark as well as the relationship between the number of $[Ca^{2+}]$i transients and zinc sparks in different systems remains an active area of research.

We have now established that bovine eggs release zinc sparks following activation, likely originating from cortically localized $Zn^{2+}$-enriched vesicles. Studies in bovine have the

potential for dual impact -on both human and livestock reproductive health. For example, zinc insufficiency in the maternal diet during the periovulatory period can influence ovarian function and embryonic development in a mouse model and whether this translates into the settings of clinical ART or agriculture warrants further investigation [[11], [12], [13]]. Animal models of human disease are often employed to examine processes that are difficult to study in the human system. This is particularly relevant in the field of human reproductive biology, where sample availability and regulations limit the feasibility of studies in human eggs [[62], [63], [64]]. Since the development of IVF, there has been little improvement in the overall fertilization rate of oocytes collect; moreover, ART in women over 40 largely relies on donor eggs [65,66]. To increase ART success rates, multiple embryo transfers are performed routinely, which has resulted in the economic and public health burden of multiple gestations. Moreover, children born by ART procedures are at a small but significantly increased risk of imprinting disorders [67,68]. This impediment in the field is largely because of difficulties in studying the human follicle and gamete; ovaries with immature follicles are rarely harvested from young women except under the extraordinary circumstances of fertility preservation for cancer patients [[69], [70], [71]]. Moreover, although the mouse is an important model for many human conditions, including reproductive ones, the female mouse gamete is markedly different from the human. Further studies into the connection between zinc spark profiles and embryo development in bovine from more controlled populations are particularly relevant, as they will help determine if this correlation extends to larger, monoovulatory species.

## Supplementary Material

Refer to Web version on PubMed Central for supplementary material.

## Acknowledgements

We thank Jennifer Pahnke, MS, Alexander Gunn, BS, and Amanda Bayer, BS for their technical assistance with these experiments. We thank Mr. Marvin Doty for assistance with the acquisition of bovine ovaries and Dr. Nancy D/Cruz (Monash) for providing full-length bPLC-ζ.

Funding

This work was supported by research grants from Ferring Pharmaceuticals, the Center for Reproductive Health After Disease (P50 HD076188, TKW) from the National Centers for Translational Research in Reproduction and Infertility (NCTRI), the NIH (R01 GM115848 and RO1 GM038784, TVO), and NIFA (MAS00439, RAF). Use of the Advanced Photon Source, an Office of Science User Facility operated for the U.S. Department of Energy (DOE) Office of Science by Argonne National Laboratory, was supported by the U.S. DOE under Contract No. DE-AC02–06CH11357.

## References

1. Bernhardt ML, Kim AM, O'Halloran TV, Woodruff TK. Zinc requirement during meiosis I-meiosis II transition in mouse oocytes is independent of the MOS-MAPK pathway. Biol Reprod, 84 (2011), pp. 526–536 [PubMed: 21076080]
2. Bernhardt ML, Kong BY, Kim AM, O'Halloran TV, Woodruff TK. A zinc-dependent mechanism regulates meiotic progression in mammalian oocytes. Biol Reprod, 86 (2012), p. 114. [PubMed: 22302686]
3. Duncan FE, Que EL, Zhang N, Feinberg EC, O'Halloran TV, Woodruff TK. The zinc spark is an inorganic signature of human egg activation. Sci Rep, 6 (2016), p. 24737 [PubMed: 27113677]

4. Kim AM, Bernhardt ML, Kong BY, Ahn RW, Vogt S, Woodruff TK, et al. Zinc sparks are triggered by fertilization and facilitate cell cycle resumption in mammalian eggs. ACS Chem Biol, 6 (2011), pp. 716–723 [PubMed: 21526836]
5. Kim AM, Vogt S, O'Halloran TV, Woodruff TK. Zinc availability regulates exit from meiosis in maturing mammalian oocytes. Nat Chem Biol, 6 (2010), pp. 674–681 [PubMed: 20693991]
6. Kong BY, Bernhardt ML, Kim AM, O'Halloran TV, Woodruff TK. Zinc maintains prophase I arrest in mouse oocytes through regulation of the MOS-MAPK pathway. Biol Reprod, 87 (11) (2012), pp. 1–2
7. Kong BY, Duncan FE, Que EL, Kim AM, O'Halloran TV, Woodruff TK. Maternally-derived zinc transporters ZIP6 and ZIP10 drive the mammalian oocyte-to-egg transition. Mol Hum Reprod, 20 (2014), pp. 1077–1089. [PubMed: 25143461]
8. Kong BY, Duncan FE, Que EL, Xu Y, Vogt S, O'Halloran TV, et al. The inorganic anatomy of the mammalian preimplantation embryo and the requirement of zinc during the first mitotic divisions. Dev Dynam, 244 (2015), pp. 935–947.
9. Que EL, Bleher R, Duncan FE, Kong BY, Gleber SC, Vogt S, et al. Quantitative mapping of zinc fluxes in the mammalian egg reveals the origin of fertilization-induced zinc sparks. Nat Chem, 7 (2015), pp. 130–139 [PubMed: 25615666]
10. Suzuki T, Yoshida N, Suzuki E, Okuda E, Perry AC. Full-term mouse development by abolishing $Zn^{2+}$-dependent metaphase II arrest without $Ca^{2+}$ release. Development, 137 (2010), pp. 2659–2669. [PubMed: 20591924]
11. Tian X, Anthony K, Neuberger T, Diaz FJ. Preconception zinc deficiency disrupts postimplantation fetal and placental development in mice. Biol Reprod, 90 (2014), p. 83. [PubMed: 24599289]
12. Tian X, Diaz FJ. Zinc depletion causes multiple defects in ovarian function during the periovulatory period in mice. Endocrinology, 153 (2012), pp. 873–886. [PubMed: 22147014]
13. Tian X, Diaz FJ. Acute dietary zinc deficiency before conception compromises oocyte epigenetic programming and disrupts embryonic development. Dev Biol, 376 (2013), pp. 51–61 [PubMed: 23348678]
14. Zhang N, Duncan FE, Que EL, O'Halloran TV, Woodruff TK. The fertilization-induced zinc spark is a novel biomarker of mouse embryo quality and early development. Sci Rep, 6 (2016), p. 22772 [PubMed: 26987302]
15. Mendoza AD, Woodruff TK, Wignall SM, O'Halloran TV. Zinc availability during germline development impacts embryo viability in Caenorhabditis elegans. Comp Biochem Physiol C Toxicol Pharmacol, 191 (2017), pp. 194–202 [PubMed: 27664515]
16. Jeon Y, Yoon JD, Cai L, Hwang SU, Kim E, Zheng Z, et al. Zinc deficiency during in vitro maturation of porcine oocytes causes meiotic block and developmental failure. Mol Med Rep, 12 (2015), pp. 5973–5982 [PubMed: 26238161]
17. Lee K, Davis A, Zhang L, Ryu J, Spate LD, Park KW, et al. Pig oocyte activation using a Zn(2)(+) chelator, TPEN. Theriogenology, 84 (2015), pp. 1024–1032 [PubMed: 26143360]
18. Zhao MH, Kim NH, Cui XS. Zinc depletion activates porcine metaphase II oocytes independently of the protein kinase C pathway. In Vitro Cell Dev Biol Anim, 50 (2014), pp. 945–951 [PubMed: 25107407]
19. Zhao MH, Kwon JW, Liang S, Kim SH, Li YH, Oh JS, et al. Zinc regulates meiotic resumption in porcine oocytes via a protein kinase C-related pathway. PLoS One, 9 (2014), Article e102097
20. Que EL, Duncan FE, Bayer AR, Philips SJ, Roth EW, Bleher R, et al. Zinc sparks induce physiochemical changes in the egg zona pellucida that prevent polyspermy. Integr Biol (2017)
21. Tokuhiro K, Dean J. Glycan-independent gamete recognition triggers egg zinc sparks and ZP2 cleavage to prevent polyspermy. Developmental cell. (2018)
22. Adams GP, Singh J, Baerwald AR. Large animal models for the study of ovarian follicular dynamics in women. Theriogenology, 78 (2012), pp. 1733–1748 [PubMed: 22626769]
23. Malhi PS, Adams GP, Singh J. Bovine model for the study of reproductive aging in women: follicular, luteal, and endocrine characteristics. Biol Reprod, 73 (2005), pp. 45–53 [PubMed: 15744017]

24. Griffin J, Emery BR, Huang I, Peterson CM, Carrell DT. Comparative analysis of follicle morphology and oocyte diameter in four mammalian species (mouse, hamster, pig, and human). J Exp Clin Assist Reprod, 3 (2006), p. 2 [PubMed: 16509981]
25. Otoi T, Yamamoto K, Koyama N, Tachikawa S, Suzuki T. Bovine oocyte diameter in relation to developmental competence. Theriogenology, 48 (1997), pp. 769–774 [PubMed: 16728170]
26. Brunet S, Verlhac MH. Positioning to get out of meiosis: the asymmetry of division. Hum Reprod Update, 17 (2011), pp. 68–75 [PubMed: 20833637]
27. Li GP, Liu Y, Bunch TD, White KL, K.l. Aston. Asymmetric division of spindle microtubules and microfilaments during bovine meiosis from metaphase I to metaphase III. Mol Reprod Dev, 71 (2005), pp. 220–226 [PubMed: 15791589]
28. Sathananthan AH. Ultrastructure of the human egg. Hum Cell, 10 (1997), pp. 21–38 [PubMed: 9234062]
29. Lefievre L, Conner SJ, Salpekar A, Olufowobi O, Ashton P, Pavlovic B, et al. Four zona pellucida glycoproteins are expressed in the human. Hum Reprod, 19 (2004), pp. 1580–1586 [PubMed: 15142998]
30. Topper EK, Kruijt L, Calvete J, Mann K, Topfer-Petersen E, Woelders H. Identification of bovine zona pellucida glycoproteins. Mol Reprod Dev, 46 (1997), pp. 344–350 [PubMed: 9041137]
31. Ceko MJ, Hummitzsch K, Bonner WM, Aitken JB, Spiers KM, Rodgers RJ, et al. Localization of the trace elements iron, zinc and selenium in relation to anatomical structures in bovine ovaries by X-ray fluorescence imaging. Microscopy and microanalysis : the official journal of microscopy society of America, microbeam analysis society, microscopical society of Canada, vol. 21 (2015), pp. 695–705
32. Ceko MJ, Hummitzsch K, Hatzirodos N, Rodgers RJ, Harris HH. Quantitative elemental analysis of bovine ovarian follicles using X-ray fluorescence imaging. Metallomics : Integrated Biometal Sei, 7 (2015), pp. 828–836.
33. Anchordoquy JM, Anchordoquy JP, Sirini MA, Picco SJ, Peral-Garcia P, Furnus CC. The importance of having zinc during in vitro maturation of cattle cumulus-oocyte complex: role of cumulus cells. Reprod Dornest Anim = Zuchthygiene, 49 (2014), pp. 865–874. [PubMed: 25131826]
34. Picco SJ, Anchordoquy JM, de Matos DG, Anchordoquy JP, Seoane A, Mattioli GA, et al. Effect of increasing zinc sulphate concentration during in vitro maturation of bovine oocytes. Theriogenology, 74 (2010), pp. 1141–1148 [PubMed: 20688367]
35. Schneider CA, Rasband WS, Eliceiri KW. NIH Image to ImageJ: 25 years of image analysis. Nat Methods, 9 (2012), pp. 671–675 [PubMed: 22930834]
36. Vogt S. MAPS : a set of software tools for analysis and visualization of 3D X-ray fluorescence data sets. J Phys IV France, 104 (2003), pp. 635–638
37. Fissore RA, Dobrinsky JR, Balise JJ, Duby RT, Robl JM. Patterns of intracellular $Ca^{2+}$ concentrations in fertilized bovine eggs. Biol Reprod, 47 (1992), pp. 960–969. [PubMed: 1493184]
38. Yoon SY, Jellerette T, Salicioni AM, Lee HC, Yoo MS, Coward K, et al. Human sperm devoid of PLC, zeta 1 fail to induce Ca($^{2+}$) release and are unable to initiate the first step of embryo development. J Clin Invest, 118 (2008), pp. 3671–3681 [PubMed: 18924610]
39. Parrish JJ, Susko-Parrish J, Winer MA, First NL. Capacitation of bovine sperm by heparin. Biol Reprod, 38 (1988), pp. 1171–1180 [PubMed: 3408784]
40. Kurokawa M, Fissore RA. ICSI-generated mouse zygotes exhibit altered calcium oscillations, inositol 1,4,5-trisphosphate receptor-1 down-regulation, and embryo development. Mol Hum Reprod, 9 (2003), pp. 523–533 [PubMed: 12900511]
41. Malcuit C, Maserati M, Takahashi Y, Page R, Fissore RA Intracytoplasmic sperm injection in the bovine induces abnormal [$Ca^{2+}$]i responses and oocyte activation. Reprod Fertil Dev, 18 (2006), pp. 39–51. [PubMed: 16478601]
42. Chatot CL, Ziomek CA, Bavister BD, Lewis JL, Torres I. An improved culture medium supports development of random-bred 1-cell mouse embryos in vitro. J Reprod Fertil, 86 (1989), pp. 679–688 [PubMed: 2760894]

43. Kimura Y, Yanagimachi R, Kuretake S, Bortkiewicz H, Perry AC, Yanagimachi H. Analysis of mouse oocyte activation suggests the involvement of sperm perinuclear material. Biol Reprod, 58 (1998), pp. 1407–1415 [PubMed: 9623599]
44. Aguila L, Felmer R, Arias ME, Navarrete F, Martin-Hidalgo D, Lee HC, et al. Defective sperm head decondensation undermines the success of ICSI in the bovine. Reproduction, 154 (2017), pp. 307–318 [PubMed: 28751536]
45. Martell AE, Smith RM, Motekaitis RJ. Standard reference data program (national Institute of standards and technology (U.S.)) NIST critically selected stability constants of metal complexes. (6th ed), U.S. Dept, of Commerce. National Institute of Standards and Technology, Standard Reference Data Program, Gaithersburg, Md (2001)
46. Loi P, Ledda S, Fulka J Jr., Cappai P, Moor RM. Development of parthenogenetic and cloned ovine embryos: effect of activation protocols. Biol Reprod, 58 (1998), pp. 1177–1187 [PubMed: 9603251]
47. Schultz RM. From egg to embryo: a peripatetic journey. Reproduction, 130 (2005), pp. 825–828 [PubMed: 16322542]
48. Ito J, Parrington J, Fissore RA. PLCzeta and its role as a trigger of development in vertebrates. Mol Reprod Dev, 78 (2011), pp. 846–853 [PubMed: 21823187]
49. Ross PJ, Beyhan Z, Iager AE, Yoon SY, Malcuit C, Schellander K, et al. Parthenogenetic activation of bovine oocytes using bovine and murine phospholipase C zeta. BMC Dev Biol, 8 (2008)
50. Ross PJ, Rodriguez RM, Lager AE, Beyhan Z, Wang K, Ragina NP, et al. Activation of bovine somatic cell nuclear transfer embryos by PLCZ cRNA injection. Reproduction, 137 (2009), pp. 427–437 [PubMed: 19074500]
51. Yoon SY, Eum JH, Lee JE, Lee HC, Kim YS, Han JE, et al. Recombinant human phospholipase C zeta 1 induces intracellular calcium oscillations and oocyte activation in mouse and human oocytes. Hum Reprod, 27 (2012), pp. 1768–1780 [PubMed: 22456923]
52. Ducibella T, Schultz RM, Ozil JP. Role of calcium signals in early development. Semin Cell Dev Biol, 17 (2006), pp. 324–332 [PubMed: 16580237]
53. Ozil JP, Banrezes B, Toth S, Pan H, Schultz RM. $Ca^{2+}$ oscillatory pattern in fertilized mouse eggs affects gene expression and development to term. Dev Biol, 300 (2006), pp. 534–544 [PubMed: 16996050]
54. Ozil JP, Markoulaki S, Toth S, Matson S, Banrezes B, Knott JG, et al. Egg activation events are regulated by the duration of a sustained $[Ca^{2+}]$cyt signal in the mouse. Dev Biol, 282 (2005), pp. 39–54 [PubMed: 15936328]
55. Fissore RA, Kurokawa M, Knott J, Zhang M, Smyth J. Mechanisms underlying oocyte activation and postovulatory ageing. Reproduction, 124 (2002), pp. 745–754 [PubMed: 12530912]
56. Gordo AC, Rodrigues P, Kurokawa M, Jellerette T, Exley GE, Warner C, et al. Intracellular calcium oscillations signal apoptosis rather than activation in in vitro aged mouse eggs. Biol Reprod, 66 (2002), pp. 1828–1837 [PubMed: 12021069]
57. Sanfins A, Lee GY, Plancha CE, Overstrom EW, Albertini DF. Distinctions in meiotic spindle structure and assembly during in vitro and in vivo maturation of mouse oocytes. Biol Reprod, 69 (2003), pp. 2059–2067 [PubMed: 12930715]
58. Sanfins A, Plancha CE, Overstrom EW, Albertini DF. Meiotic spindle morphogenesis in in vivo and in vitro matured mouse oocytes: insights into the relationship between nuclear and cytoplasmic quality. Hum Reprod, 19 (2004), pp. 2889–2899 [PubMed: 15388682]
59. Liu XY, Mal SF, Miao DQ, Liu DJ, Bao S, Tan JH. Cortical granules behave differently in mouse oocytes matured under different conditions. Hum Reprod, 20 (2005), pp. 3402–3413 [PubMed: 16172151]
60. Lee HC, Yoon SY, Lykke-Hartmann K, Fissore RA, Carvacho I.TRPV3 channels mediate Ca(2)(+) influx induced by 2-APB in mouse eggs. Cell Calcium, 59 (2016), pp. 21–31 [PubMed: 26725171]
61. Swann K, Saunders CM, Rogers NT, Lai FA. PLCzeta(zeta): a sperm protein that triggers $Ca^{2+}$ oscillations and egg activation in mammals. Semin Cell Dev Biol, 17 (2006), pp. 264–273 [PubMed: 16730199]

62. Rodriguez S, Campo-Engelstein L, Tingen C, Woodruff T. An obscure rider obstructing science: the conflation of parthenotes with embryos in the Dickey-Wicker amendment. Am J Bioeth, 11 (2011), pp. 20–28

63. Tingen C, Rodriguez S, Campo-Engelstein L, Woodruff TK. Research funding. Politics and parthenotes. Science, 330 (2010), p. 453 [PubMed: 20966235]

64. Campo-Engelstein L, Rodriguez S, Tingen C, Woodruff T. Practical parthenote policy and the practice of science. Am J Bioeth, 11 (2011), pp. W1–W2

65. Benagiano G, Farris M, Grudzinskas G. Fate of fertilized human oocytes. Reprod Biomed Online, 21 (2010), pp. 732–741 [PubMed: 21050816]

66. Bromer JG, Sakkas D, Siano LJ, Benadiva CA, Patrizio P. Reproductive efficiency of women over the age of 40 and the low risk of multiple pregnancies. Reprod Biomed Online, 19 (Suppl 4) (2009), p. 4316 [PubMed: 20034414]

67. Dupont C, Sifer C. A review of outcome data concerning children born following assisted reproductive Technologies. ISRN Obstet Gynecol, 2012 (2012), p. 405382 [PubMed: 22778982]

68. Thompson JR, Williams CJ. Genomic imprinting and assisted reproductive technology: connections and potential risks. Semin Reprod Med, 23 (2005), pp. 285–295 [PubMed: 16059835]

69. Woodruff TK. Preserving fertility during cancer treatment. Nat Med, 15 (2009), pp. 1124–1125 [PubMed: 19812566]

70. Woodruff TK. From the bench to bedside to babies: translational medicine made possible by funding multidisciplinary team science. J Assist Reprod Genet, 30 (2013), pp. 1249–1253 [PubMed: 23975192]

71. Duncan FE, Jozefik JK, Kim AM, Hirshfeld-Cytron J, Woodruff TK. The gynecologist has a unique role in providing oncofertility care to young cancer patients.US Obstet Gynecol, 6 (2011), pp. 24–34 [PubMed: 21927621]

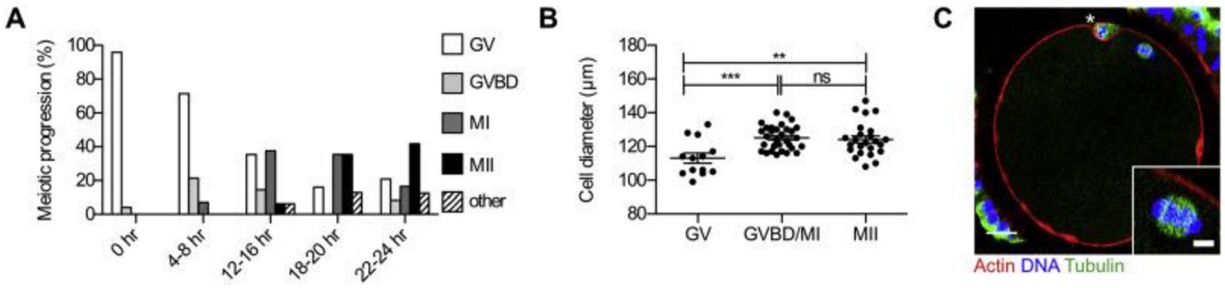


**Fig. 1.**

Characteristics of bovine eggs obtained through in vitro maturation (IVM). (a) The percent of bovine oocytes at each stage of meiosis (scored by chromatin configuration) following specific times of IVM. (b) Average diameter of bovine eggs at different meiotic stages following IVM (**, $p = 0.0037$; ***, $p < 0.0001$; ns, not significant). (c) Bovine eggs arrested at metaphase of meiosis II were fixed and stained for actin, tubulin, and DNA to assess cytoskeleton morphology (Scale bars, 20 µm). A representative image is shown, and the meiotic MII spindle is highlighted in the inset. The asterisk marks the first polar body.

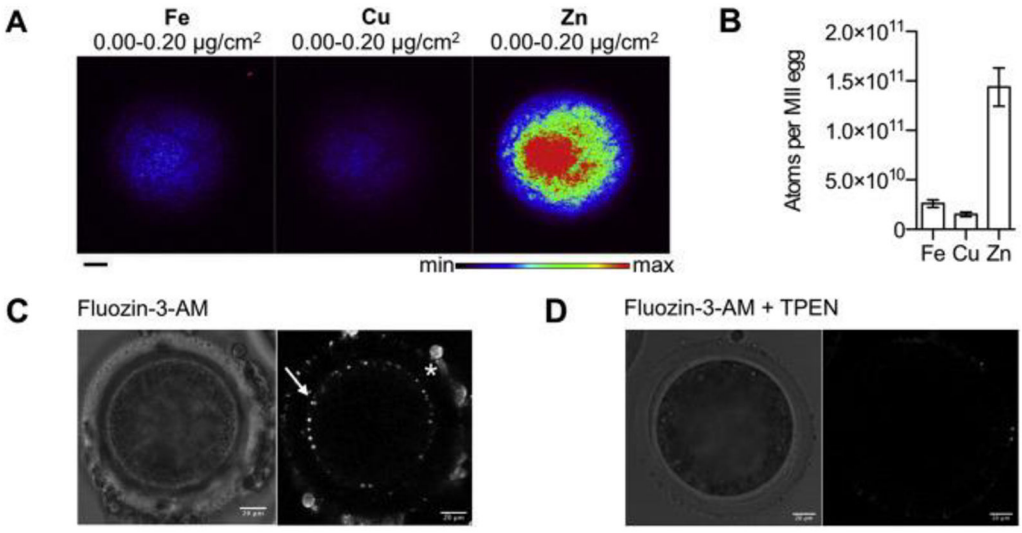


**Fig. 2.**

Zinc is abundant in bovine eggs and labile zinc is localized to cortical structures. (a) X-ray fluorescence microscopy (XFM) elemental maps were obtained for bovine MII eggs (n = 13). Representative images are shown. Uniform distributions of Fe, Cu, and Zn are observed. The minimum and maximum elemental threshold values are shown above each image. (b) Quantification of the number of Fe, Cu, and Zn atoms in bovine MII eggs. Zn was present in significantly higher quantities (1.4 × 1011 atoms/cell) than Fe (2.6 × 1010 atoms/cell) and Cu (1.5 × 1010 atoms/cell) ($p < 0.0001$). Average elemental content ± SEM (standard error of the mean) are displayed. (c) Live cell fluorescence image of a bovine MII egg stained with 5 µM FluoZin-3 AM. Fluorescence is observed in cortical structures (arrow) and in cumulus cells attached to the zona pellucida (*). Image represents an optical section imaged near the middle of the egg. (d) Live cell fluorescence image of the same cell after treatment with the $Zn^{2+}$ chelator TPEN (N,N,N′,N′-tetrakis(2-pyridylmethyl)ethane-1,2-diamine, 10 µM), for 30 min where the fluorescence signal is greatly reduced. All scale bars, 20 µm.

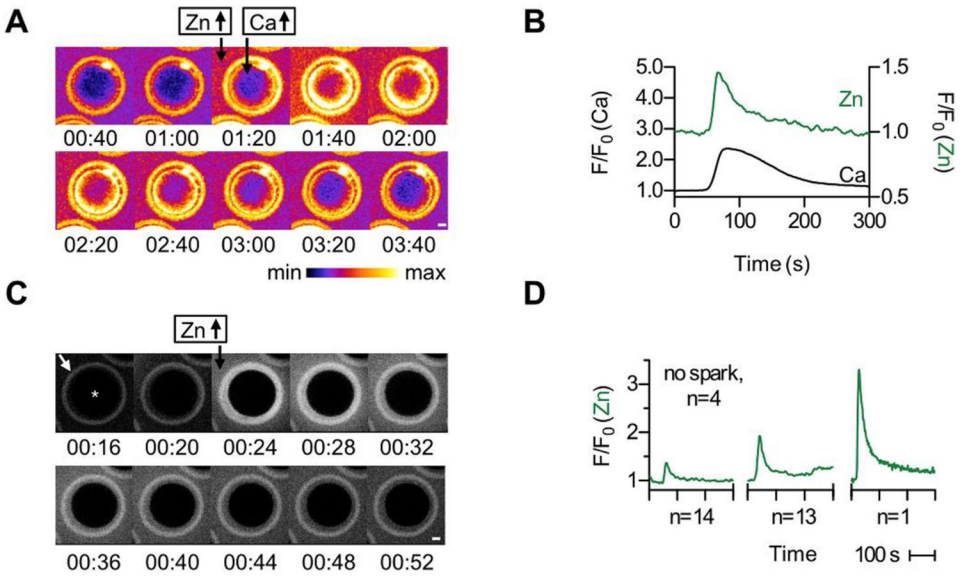


**Fig. 3.**

Ionomycin treatment induces a zinc spark in bovine eggs. (a) Time course montage of $Zn^{2+}$ and $Ca^{2+}$ fluxes in a bovine egg treated with 50 μM Ca-ionomycin. Extracellular $Zn^{2+}$ and intracellular $Ca^{2+}$ were monitored using 50 μM FZ3 and 5 μM Fluo4-AM (Fluo4) respectively. (b) Representative time traces of normalized Fluo4 (black) and FZ3 (green) fluorescence. $Zn^{2+}$ release occurs simultaneously with the rise in $[Ca^{2+}]i$ within the experimental time resolution (2 s). Scale bars, 20 μm. (c) Time course montage of $Zn^{2+}$ release from a bovine egg treated with 50 μM Ca-ionomycin. Extracellular $Zn^{2+}$ was monitored using 50 μM Fluozin-3 (FZ3). We note that the zona pellucida in these cells contains enhanced Fluozin-3 fluorescence, as is seen in the ring structure (white arrow, leftmost panel) surrounding the main body of the egg (*). (d) Representative time traces of normalized FZ3 extracellular fluorescence (F/F0) showing the range of signal intensities observed. Of the 33 eggs monitored, 14 displayed a small spark intensity, 13 displayed a medium spark intensity, 1 displayed a large spark intensity, and 4 did not spark. Please see Videos S1 and S2 for live imaging of zinc sparks. (For interpretation of the references to colour in this figure legend, the reader is referred to the Web version of this article.)

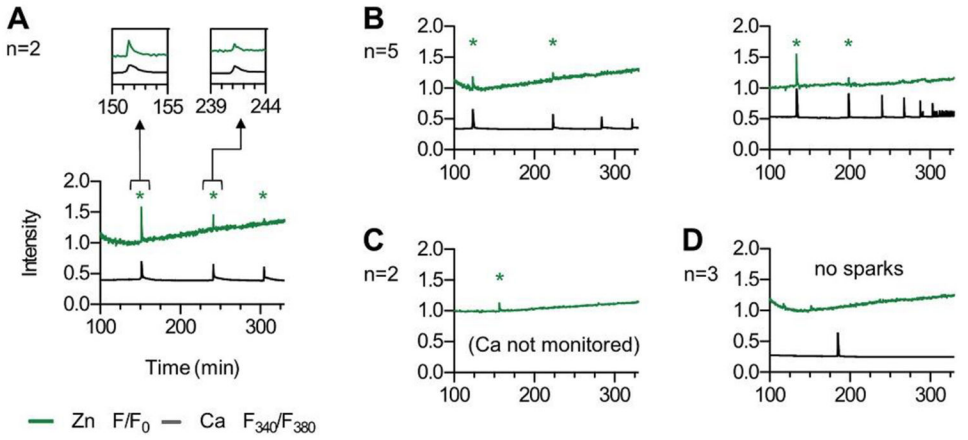


**Fig. 4.**

Activation by PLC-ζ induces multiple zinc sparks in bovine eggs. Bovine MII eggs (n = 12) were activated by injection with 0.5 μg/μL bPLCZ1 cDNA. Extracellular $Zn^{2+}$ was monitored using 50 μM FZ3. In 8/12 of the eggs, $[Ca^{2+}]i$ was monitored using Fura2-dextran (Fura2). Time traces of intensities for FZ3 (normalized F/F0, green) and Fura2 (F340/F380 ratio, black) are shown for representative samples. The x-axis represents time after bPLCZ1 injection and traces include first calcium transient. Eggs displayed three (a, n = 2), two (b, n = 5), one (c, n = 2) and zero (d, n = 3) zinc sparks (*). $Zn^{2+}$ release correlates with rises in intracellular $Ca^{2+}$ (see insets, panel a). (For interpretation of the references to colour in this figure legend, the reader is referred to the Web version of this article.)

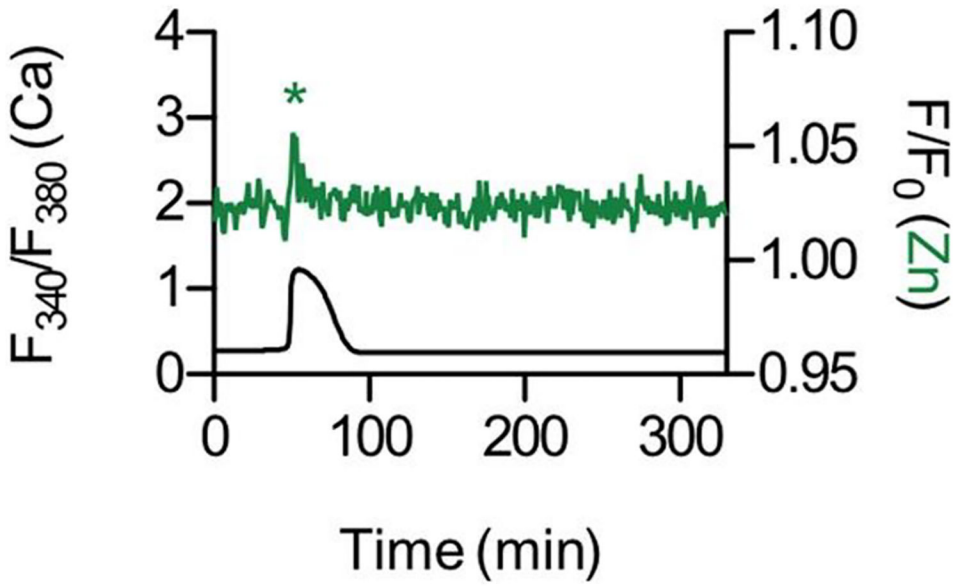


**Fig. 5.**

Intracytoplasmic sperm injection in bovine eggs induces the zinc spark. Time traces of intensities for FZ3 (normalized F/F0, green) and Fura2 (F340/F380 ratio, black) are shown for a bovine egg that was injected with multiple sperm heads. The x-axis represents time after sperm injection. The $Zn^{2+}$ release correlates to a rise in intracellular $Ca^{2+}$. (For interpretation of the references to colour in this figure legend, the reader is referred to the Web version of this article.)